

Effect of Stacking Faults on the Thermoelectric Figure of Merit of Si Nanowires

Kantawong Vuttivorakulchai*, Mathieu Luisier, and Andreas Schenk
Integrated Systems Laboratory, ETH Zürich, Gloriastrasse 35, CH-8092 Zürich, Switzerland
*email: kvuttivo@iis.ee.ethz.ch

Abstract

The efficiency of converting waste heat to electricity requires a large value of the thermoelectric figure of merit (ZT). This can be achieved by patterning bulk material into nanostructures like nanowires (NWs). Further improvement results from an increased surface roughness (SR) of such NWs [1]. In this work, Si NWs with stacking faults (SFs) are studied. It is shown that SFs can significantly reduce the lattice thermal conductivity as compared to ideal NWs [2]. A recent derivation of the phonon relaxation time for SF scattering [3] is adapted to the electronic case. It turns out that in most cases the thermoelectric power factor (PF) decreases to a lesser extent than the thermal conductivity. This can double ZT provided that SR scattering of electrons is negligible.

Introduction

It has been shown experimentally that the presence of SFs strongly increases the ZT value of InAs NWs with a diameter of 20 nm [4]. To the best of our knowledge, such experiments have not been conducted yet with Si NWs, where SFs arise as the interfaces between alternating regions having either diamond (DM) or wurtzite (WZ) structure. For the first time, the simulation of such a Si NW with 70 nm in diameter will be presented.

Approach

First-principle calculations based on projector augmented-wave (PAW) pseudopotentials with hybrid functional of Heyd, Scuseria, and Ernzerhof (HSE06) [5] as implemented in the Vienna *ab initio* simulation package (VASP) were performed [6,7]. The electronic band structures are calculated for the cubic unit cells of DM oriented in $\langle 100 \rangle$ and $\langle 111 \rangle$ direction, respectively, and WZ oriented in $\langle 0001 \rangle$ direction along the x -axis. These band structures are the input for our in-house linearized Boltzmann transport equation (BTE) solver. The SF scattering model developed for phonons in Ref. [3] is modified for electron scattering at SFs. Only an exponential distribution of SFs is considered here, and the average distance between SFs (l_{sf}) along the NW is assumed to be 2.5 nm. The computation of the electronic relaxation time for SF scattering requires the knowledge of the energy difference between DM in $\langle 111 \rangle$ direction and WZ in $\langle 0001 \rangle$ direction (see Fig. 1). The number of atoms must be the same in both lattice configurations, hence two (three) smallest unit cells of DM (WZ) are used. For a dense k -point sampling in the BTE calculation, the first Brillouin zone is discretized by 401 points in x -direction and 101 points in the other directions.

Apart from SF scattering, the electronic relaxation time is determined by electron-phonon scattering as shown in Fig. 2. Band parameters of Si as given in Ref. [8] are used. SR scattering and all kinds of Coulomb scattering are ignored. The electron density is treated as a parameter. The possible impact of SR scattering would de-

pend on the surface field that emerges as the electrostatic consequence of doping, interface charges, and fixed oxide charges. A doping level of $\sim 1 \times 10^{20} \text{ cm}^{-3}$ as chosen in Ref. [9] generates flat-band conditions and makes SR scattering a second-order effect in bulk-like NWs.

Results

Near the conduction band edge, the energetic rate of SF scattering strongly dominates over the rate of electron-phonon scattering (Fig. 2). The latter becomes stronger when the energy increases. The figure of merit ZT is the product of PF and average temperature between two contacts, divided by the sum of lattice and electron thermal conductivities. The PF is given by the square of the Seebeck coefficient (S) multiplied by the electrical conductivity. As shown in Fig. 3(a), the calculated S of the DM structure perfectly fits the experimental data. As $|S|$ is the conductance-averaged energy difference $|E - E_F|$, it decreases with increasing density. The electron mobility of the DM structure oriented in $\langle 100 \rangle$ -direction matches the measured bulk electron mobility for negligible doping concentration ($< 10^{12} \text{ cm}^{-3}$) as can be seen in Fig. 3(b). However, the mobility of the DM structure oriented in $\langle 111 \rangle$ -direction has smaller values as function of both temperature and electron concentration (see Fig. 3(c)). The structure with SFs exhibits a clear reduction of the electron mobility compared to the two DM structures.

Calculations of the lattice thermal conductivity of bulk Si and Si NWs are reproduced from Ref. [2] in Fig. 4(a). As in the case of InAs NWs [3], comparable reductions of the thermal conductivity of Si NWs can be obtained with SFs instead of SR. Figure 4(b) shows the PF as function of electron density at 300 K and 500 K. SFs lower the PF significantly over the entire concentration range. The percentage reduction of the PF of Si NWs as the consequence of SFs reduces when the temperature increases. The ZT as function of electron concentration is presented in Fig. 4(c). As expected, engineering NWs increases the ZT value compared to the bulk case. The benefit of SFs to the improvement of ZT is clearly observed in the high-density range and at high temperatures. A doubling of the ZT value compared to that of an ideal NW could be achievable.

Conclusion

An in-house linearized BTE solver was used to derive the ZT of bulk Si, ideal Si NWs, and Si NWs with SFs based on DFT band structure calculations for electrons and phonons. NWs with SFs have a lower electron mobility and a smaller PF. At high electron concentration, this suppression is reduced by the increasing role of electron-phonon scattering, whereas the lattice thermal conductivity remains the same. This leads to an improved ZT. Our simulations show the possibility of engineering the ZT of Si NWs by the introduction of SFs. This could encourage experimentalists to explore the benefit of such NWs for thermoelectric converters.

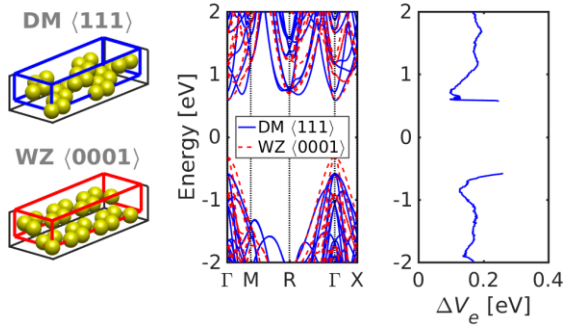


Figure 1: Left panel: Schematic view of the two (three) smallest cubic unit cells of DM (WZ) in $\langle 111 \rangle$ ($\langle 0001 \rangle$) direction. Right panel: The corresponding electronic band structures calculated by density functional theory (DFT) and the energy difference between DM and WZ structures. A k -point sampling of " $401 \times 101 \times 101$ " is used.

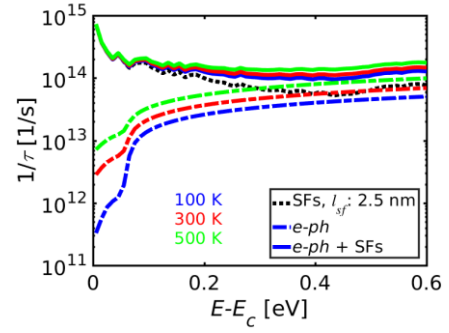


Figure 2: Energetic scattering rate of electrons from different scattering mechanisms, i.e. electron-phonon (e - ph) scattering and SF scattering with l_{sf} equal to 2.5 nm, at different temperatures. The energy zero is the conduction band edge (E_c).

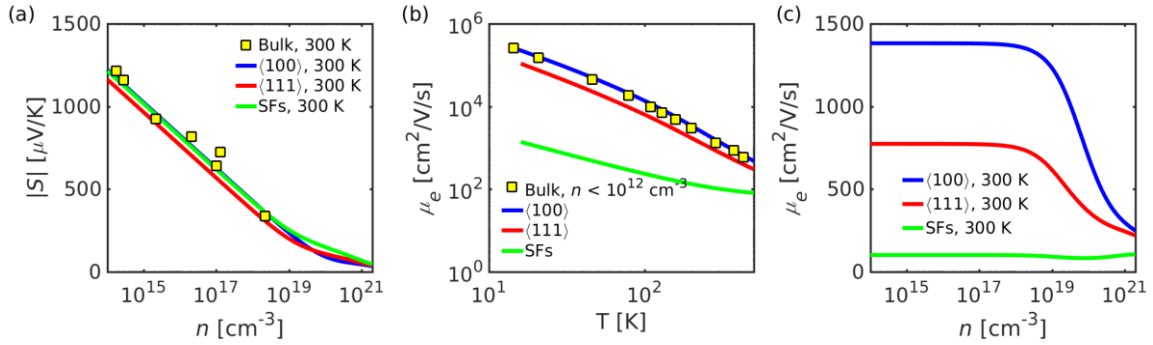


Figure 3: (a) Absolute value of Seebeck coefficient as function of electron concentration (n) at room temperature. The blue (red) line corresponds to a cubic unit cell of DM oriented in $\langle 100 \rangle$ ($\langle 111 \rangle$) direction, respectively. Symbols represent the experimental data of Ref. [10]. (b) Electron mobility as function of temperature at an electron concentration of 10^{12} cm^{-3} . Symbols are experimental data from Ref. [11]. (c) Electron mobility as function of electron concentration at 300 K.

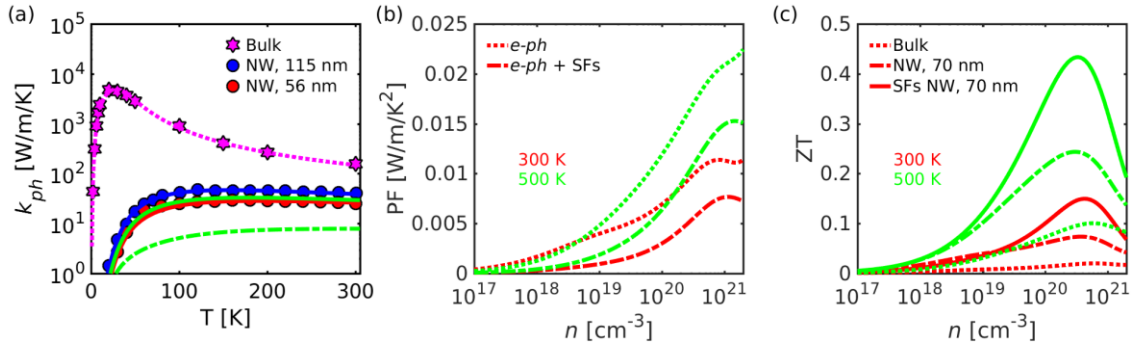


Figure 4: (a) Lattice thermal conductivity as function of temperature. Symbols denote the measurements from Refs. [1,12-13]. Lines are simulated thermal conductivities. The dotted line is for the bulk case, whereas solid lines are for the ideal NW case. The dash-dotted line is for a NW with SFs. Blue (green, red) lines are for 120 nm (70 nm, 56 nm) diameter, respectively. (b) Power factor as function of electron density with temperatures equal to 300 K and 500 K. (c) Thermoelectric figure of merit as function of electron density of bulk (dotted), ideal NW (dashed), and NW with SFs (solid). The NW diameter is 70 nm.

References

- [1] A. I. Hochbaum et al., Nature, vol. 451, no. 7175, pp. 163-167, January 2008.
- [2] K. Vuttivorakulchai et al., IWCN, May 2019, (in press).
- [3] K. Vuttivorakulchai et al., J. Appl. Phys., vol. 124, no. 20, pp. 205101, November 2018.
- [4] P. Mensch et al., Appl. Phys. Lett., vol. 106, no. 9, pp. 093101, March 2015.
- [5] J. Heyd et al., J. Chem. Phys., vol. 118, no. 18, pp. 8207-8215, April 2003.
- [6] G. Kresse et al., Phys. Rev. B, vol. 54, no. 16, pp. 11169-11186, October 1996.
- [7] J. P. Perdew et al., Phys. Rev. Lett., vol. 100, no. 13, pp. 136406, April 2008.
- [8] C. Jacoboni and L. Reggiani, Rev. Mod. Phys., vol. 55, no. 3, pp. 645-705, July 1983.
- [9] A. I. Boukai et al., Nature, vol. 451, no. 7175, pp. 168-171, January 2008.
- [10] B. Liao et al., Nat. Commun., vol. 7, pp. 13174, October 2016.
- [11] C. Jacoboni et al., Solid State Electron., vol. 20, no. 2, pp. 77-89, February 1977.
- [12] C. J. Glassbrenner and G. A. Slack, Phys. Rev., vol. 134, no. 4A, pp. A1058-A1069, May 1964.
- [13] M. G. Holland, Phys. Rev., vol. 132, no. 6 pp. 2461-2471, December 1963.